JOURNAL OF Applied Polymer SCIENCE

New Copolymer of Poly(*N*-vinylcarbazole) and Poly(p-phenylenevinylene) for Optoelectronic Devices

Mohamed Mbarek,[1] Florian Massuyeau,[2] Jean-Luc Duvail,[2] Jany Wery,[2] Eric Faulques,[2] Kamel Alimi[1]

[1]Unité de Recherche : Matériaux nouveaux et Dispositifs Electroniques Organiques (UR 11ES55), Faculté des Sciences de Monastir, Université de Monastir-Tunisie, Tunisia

[2]Institut des Matériaux Jean Rouxel, CNRS-UMR 6502, 2 Rue de la Houssinière, BP 32229, 44322 Nantes cedex 3, France

Correspondence to: K. Alimi (E-mail: kamel.alimi@fsm.rnu.tn)

ABSTRACT: A novel diblock copolymer based on poly(*N*-vinylcarbazole) PVK and poly(p-phenylenevinylene) (PPV) precursor was synthesized by oxidative cross-linking. The grafting of PPV with PVK moieties was elucidated by infrared absorption analysis. A structural study by X-ray diffraction and a morphological study of the copolymer by scanning and transmission electron microscopy reveal a multiscale one-dimensional self-organization both at the molecular and at the sub-micrometric level. The resulting copolymer exhibits original optical properties compared to those of PVK and PPV ones and presents an improved thermal behavior. © 2013 Wiley Periodicals, Inc. J. Appl. Polym. Sci. 130: 2839–2847, 2013

KEYWORDS: copolymers; grafting; optical properties

Received 24 February 2013; accepted 29 April 2013; Published online 8 June 2013
DOI: 10.1002/app.39496

INTRODUCTION

Phase-separated polymer blends often achieving nanoscale phase dimensions as block copolymer domain morphology is usually at the nanoscale level.[1] For several decades, block copolymers have received great attention. During the last years, they have been widely considered for nanotechnological applications.[2,3] Their applicability to nanotechnology stems from their specific morphology wit sub-micrometric domains, from the convenient tunability of properties for example by copolymerization,[4,5] and from periodicity afforded by changing their molecular parameters. Conjugated copolymers are widely used for application in the electronic and optoelectronic fields in order to benefit from complementary properties of their components[6,7] or for original optoelectronic behavior.[8] Poly(*N*-vinylcarbazole) PVK is one of the most interesting functional polymers,[9–15] due to its charge transfer capability,[16] its high thermal stability[17] and its conducting behavior.[18] The simple process of polymerization for PVK by an oxidative route opens opportunities for the synthesis of new copolymers.[19–21] Recently, Chemek et al.[21] prepared a new copolymer based on PVK, P3HT, and P6HT, while Melki et al.[22] have synthesized a new copolymer based on PVK and PEDOT via oxidative process. In these previous works, anhydrous $FeCl_3$ has been used as oxidant to increase the PVK polymerization and create a coupling site in the PVK skeleton.[23]

On the other hand, poly(p-phenylenevinylene) (PPV) and its derivatives have been widely used in optoelectronic devices.[24,25] One way to synthesize copolymers containing PPV moieties is to use the precursor of PPV.[26,27] The control of the conjugation length and the introduction of some functional groups make possible to tune the emission range. Most conjugated systems in light-emitting polymers consist of simple aromatic moieties. A copolymer strategy consisting in the insertion of PPV block within the N-heterocycles is relevant for the design of new conjugated systems. Thus, combining PPV blocks with carbazole units, in a copolymer is particularly attractive to benefit from both the efficient emission feature of PPV and the high hole mobility of PVK. In this regard, we synthesized a new copolymer based on PVK and PPV. The PPV precursor and the PVK have been mixed with a controlled quantity of anhydrous $FeCl_3$ to proceed to the copolymer formation. The resulting copolymer was characterized by X-rays diffraction and infrared (IR) absorption to evaluate its structure and its thermal stability. A fiber morphology both at the molecular and at the sub-micrometric scale has been elucidated by scanning and transmission electron microscopy study. Finally the optical properties have been evaluated by steady state photoluminescence and optical density measurements.

EXPERIMENTAL

Materials

Poly(*N*-vinylcarbazole) PVK powder, ferric chloride ($FeCl_3$), chloroform, methanol, and hydrazine used for the synthesis of the studied compounds were purchased from Sigma Aldrich,

Applied Polymer SCIENCE

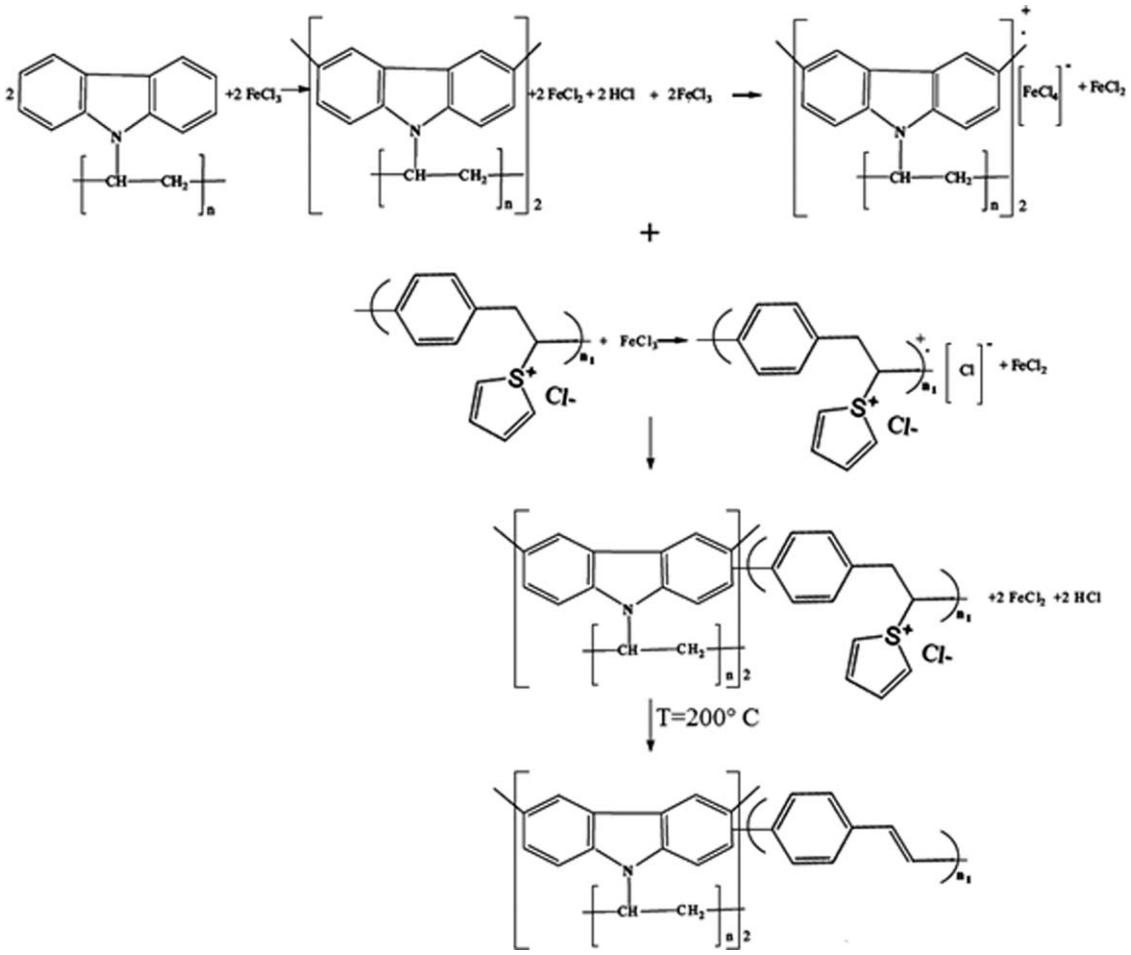

Scheme 1. Possible mechanism of the formation of graft copolymer of PVK and PPV.

Merk, and Fluka. The materials were used as received. The PPV precursor was synthesized by addition of 33 mL of tetrahydrothiophenium in the dichloroparaxylene dissolved in methanol. The aqueous solution of PPV precursor was dialyzed with deionized water for several days. The PPV precursor was kept at 0°C in the dark. The mass concentration of the PPV precursor is about 2.4 mg mL^{-1}.

Preparation of PVK-PPV Copolymer

Totally, 30 mg of PVK were dissolved in 10 mL of $CHCl_3$, with addition of 250 mg of anhydrous $FeCl_3$. 12.5 mL of PPV precursor were kept in the methanol solvent. The mixture was reserved with agitation in darkness and in an ice bath for 3 days, then kept under reflux at 55°C for 3 h and washed thoroughly with methanol. The mixture was finally dried under vacuum for 1 h at 80°C. The resulting powder is insoluble in common organic solvent. The polymerization yield of PVK-PPV precursor was evaluated to be 54.1%. Finally, the resulting copolymer was annealed at $T = 200$°C for 3 h under secondary vacuum nearly 4.6 10^{-6} mbar to ensure the full removal of THT groups, as tetra-hydrothiophene groups (THT) of PPV precursor are known to be removed within a temperature range from 75°C to 125°C.[28]

In order to determine the relationship between structure and properties, we propose in Scheme 1, the possible grafting mechanism after the cross-linking of carbazole with $FeCl_3$.

Characterization Methods

Infrared absorption spectra were measured with a Brüker Vector 22 Fourier transform spectrophotometer. Samples were prepared in pellets of KBr mixed with the organic compound. Dynamic thermo-gravimetric analysis (TGA) was performed in a Perkin-Elmer TGS-1 thermal balance with a Perkin-Elmer UV-1 temperature program control. Samples were placed in a platinum sample holder and the thermal degradation measurements were carried out between 300 and 973 K at a rate of 5 K/min under nitrogen atmosphere. The scanning electron microscopy analysis was carried out using a microscope JEOL 6400F. Transmission electron microscopy (TEM) measurements were performed in a cold FEG Hitachi HF2000 operating at 100 keV. The diffraction patterns were obtained with a SIEMENS 5000 diffractometer (wavelength Cu K α 40 kV (λ =1.5405 Å), 30 mA) in Bragg Brentano geometry. Optical density measurements were carried out at room temperature (RT) using a Cary 5000 spectrophotometer, in the range 200–2200 nm. Continuous-wave (cw) photoluminescence (PL) measurements were collected on a Jobin-Yvon Fluorolog 3 spectrometer using a Xenon lamp (500W) at room temperature. Time-resolved photoluminescence (TR-PL) experiments, at RT were acquired with a regenerative amplified femtosecond Ti:Sapphire laser system (Spectra Physics Hurricane X). This setup generates 100 fs pulses at 800 nm with a repetitive rate of 1 kHz and a power of 1W. The laser line is

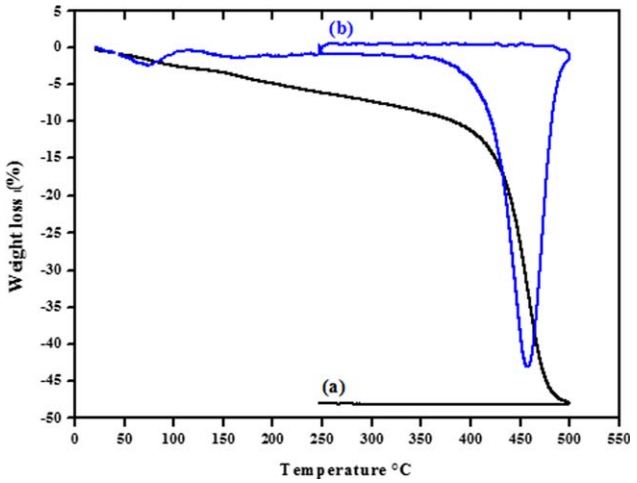

Figure 1. TGA micrograph of copolymer (a), and its derivative (b). [Color figure can be viewed in the online issue, which is available at wileyonlinelibrary.com.]

frequency-doubled with a thin BBO crystal to obtain an excitation line λ_{exc} = 400 nm (3.1 eV). The pump energy pulse is controlled to ensure that the excitation density in the sample does not exceed 10^{17} cm^{-3}, to avoid bimolecular annihilation process and sample photodegradation. TR-PL-3D-maps were obtained with energy emission versus time (range, 0–0.8 ns) and intensity in false color. The emission spectra were temporally resolved with a high dynamic range Hamamatsu C7700 streak camera coupled with an imaging spectrograph with a temporal resolution of 20 ps and processed using the HPDTA Hamamatsu software.

RESULTS AND DISCUSSION

The thermal stability of the copolymer has been evaluated. The weight loss versus temperature for the PVK-PPV copolymer (Figure 1) shows that its decomposition begins around 450°C, while the decomposition of PVK begins around 380°C[29] A very strong increase of about 70°C in the thermal stability is obtained. It can be attributed to the coplymerization with PPV because its decomposition begins at higher temperature than PVK, around 550°C.[30] Therefore, including the PPV moiety in the PVK backbone enhances the thermal stability of the new copolymer. As seen from the TGA thermogram, four steps constitute the decomposition process of the copolymer. The first one (<3% weight loss) may be related to the THT groups of precursor of PPV which occurs at 76°C. Over the temperature range 100–175°C, the second one (weight loss varying from 3% to 5%) may be attributed to the remainder of the THT groups.[28] The third copolymer decomposition starts around 400–425°C. The corresponding weight loss (10%), starting from 425°C, may be associated with the ring degradation finished by a complete decomposition at 500°C. This enhanced thermal stability additionally supports the assumption that PPV chains are incorporated into the skeleton of PVK to yield a new copolymer.

To elucidate the interactive character between both components and to gain information about the final structure, we present in Figure 2 Fourier transform infrared spectra (FT-IR) of PVK, PPV and the copolymer. All the characteristic vibrations and their changes for the copolymer relative to the PVK and PPV case are summarized in Table I. A new band appears at 794 cm^{-1} which is attributed to the benzene ring vibration, relative to the dimeric carbazylium formation under $FeCl_3$ oxidation as reported previously.[31,32] Another band appears at 813 cm^{-1} corresponding to the deformation of para-phenylene bending C-H out-of-plane of PPV.[33] In addition the band located at 1110 cm^{-1} is assigned to C-H deformation of phenylene ring of PPV. The next band at 1288 cm^{-1} is assigned to the C-H deformation in plane of vinylene groups of PPV block. Another band located at 1338 cm^{-1} is attributed to the deformation of phenylene groups of PPV. The band located at 1512 cm^{-1} is ascribed to aromatic C-C ring stretching of PPV.[33] The presence of these bands confirms the presence of PPV in the backbone of PVK. This observation confirms that the PVK polymer was inserted within PPV blocks. Moreover, some other PPV bands centred at 834 and 966 cm^{-1} and PVK bands located at 1002 and 1122 cm^{-1} are not present for the copolymer. On the other hand, the vinylcarbazole (VC) bands located at 1026 cm^{-1} and 1450 cm^{-1} decrease in intensity in the copolymer which indicates a reduction of the number of VC monomer units whereas the contribution of PPV units in the copolymer is favored. Compared to the PVK, the modification of the intensity ratio between the IR bands in the case of copolymer at 720 and 740 cm^{-1} indicates the presence of some steric hindrance effects caused by the presence of PPV segments.[34] On the whole, the

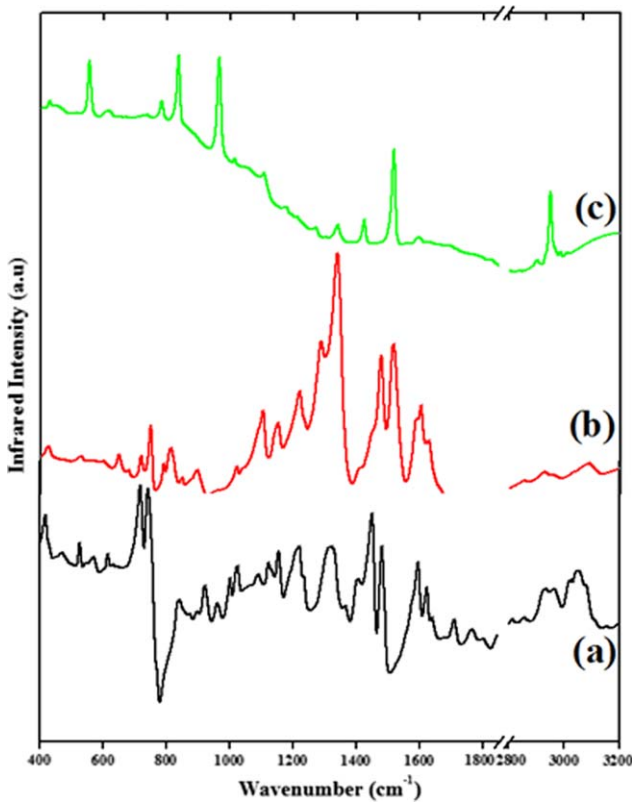

Figure 2. Infrared spectra of (a) PVK, (b) copolymer and (c) PPV. [Color figure can be viewed in the online issue, which is available at wileyonlinelibrary.com.]

Table I. Infrared Intensity and Peak Positions of PVK, Copolymer, and PPV.[30,32,33]

PVK		Copolymer		PPV		Assignments
ν (cm^{-1})	I	ν (cm^{-1})	I	ν (cm^{-1})	I	
418	M	420	w	–	–	Ring vibration
–	–	–	–	555	M	Phenyle deformation out of plane
615	V.w	613	V.w	–	–	Vibration of benzene monosubstituated
717	V.S	721	M	–	--	Ring Deformation
742	V.S	744	M	–	–	CH_2 Vibration "rocking"
–	–	–	–	783	w	CH out of plane of p-phenyle
–	–	794	M	–	–	Benzene ring vibration of dimer of PVK
–	–	813	M	–	–	C—H out of plane of phenyle of PPV
–	–	–	–	834	S	C—H out of plane of phenyle of PPV
840	M	839	M	–	–	Stretching C=C aliphatique
921	S	921	S	–	–	Vibration C—C of PVK
–	–	–	–	966	S	CH out of plane of trans vinyl group
1002	V.w	–	–	–	–	Stretching C—C of PVK
1026	V.w	–	–	–	–	Stretching C—C of PVK
–	–	1110	w	1107	w	CH deformation of phenylene ring of PPV
1121	M	–	–	–	–	C—H deformation in plane
1151	M	–	–	–	–	C—H in plane deformation of aromatic ring
1220	S	1220	S	–	–	C—N stretching
–	–	1288	M	1288	M	C—H deformation in plane of vinyl of PPV
1321	S	–	–	–	–	C—H deformation of vinylidene groups
–	–	1338	V.S	1336	V.S	Phenyle deformation of PPV
1406	M	1406	M	–	–	CH_2 deformation of vinylene group
–	–	–	–	1424	M	C—C ring stretching
1450	V.S	1456	M	–	–	Ring vibration of PVK + phenyle group of PPV
1481	M	1483	M	–	–	Antisymetric C=C stretching
–	–	1512	S	1515	S	C—C stretching of PPV
1596	S	1596	F	–	–	CH_2 stretching of PVK
1623	M	1624	w	–	–	C—C stretching du benzene
2930	V.w	2929	w	–	–	CH_2 assymetric stretching
3047	w	3051	w	–	–	CH—CH_2 assymetric stretching

I, intensity; v.w, very weak; w, weak; M, mean; S, strong; V.S, very strong.

changes observed in the IR absorption features (appearance of a new band and disappearance of PPV and PVK bands) are hints that PPV and PVK moieties may have established chemical bonding during the copolymerization reaction.

The supermolecular structure has been investigated by XRD (Figure 3). For the copolymer, the pattern is dominated by a broad peak at 13.7° and a less intense peak at about 27°. This contrasts with both the PVK and PPV XRD patterns dominated respectively by a band at 21° and at 22.5°, respectively. It can be noticed that the peak located at 13.7° is also present in PVK. These results reflect a new macromolecular regioregularity[35,36] for the copolymer with a characteristic distance evaluated to about 6.5 Å and 3.3 Å from the Bragg relation respectively for the two peaks previously described. One can assume that these distances correspond to the separation between two successive chains. This modified macromolecular regioregularity can result in a different morphology at the nano- and microscale. Moreover, the broadening of the diffraction peaks makes the precise analysis of the diffraction profile more difficult. It has been characterized by TEM and SEM. On the one hand, the TEM study clearly shows a fibrillar organization at the nanometric scale, as reported on the TEM micrograph of the copolymer (Figure 4). However, the TEM image does not evidence the presence of a high ordered inset of PVK-PPV copolymer. From TEM image, the Fast Fourier Transform was performed on those regioregular regions (yellow squares) is presented below the TEM micrographs. Interchains spaces of 7 Å, 4.4 Å, 3.8 Å and 7.4 Å were measured in the selected regioregular regions (a), (b), (c) and (d) respectively (presented with yellow squares). Those results are in agreement with the X-ray diffraction. Figure 5 shows the scanning electron micrographs of the PVK and the copolymer. A

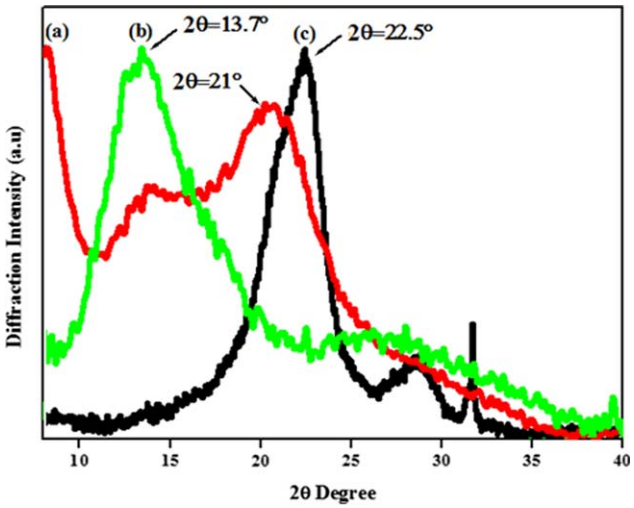

Figure 3. XRD pattern spectra of (a) PVK, (b) copolymer and (c) PPV. [Color figure can be viewed in the online issue, which is available at wileyonlinelibrary.com.]

completely different morphology can be observed, with the formation of long nanofibers for the copolymer with a nanofiber diameter in the range 66–110 nm and lengths of hundreds of nanometers as shown in Figure 6. It is proposed that this nanofiber morphology is promoted by the self-organisation of the polymer chains at the molecular level into one-dimensional structures. These dramatic changes of the structure and the morphology in the copolymer could strongly influence the charge and energy transfer properties or the exciton migration along the copolymer skeleton.

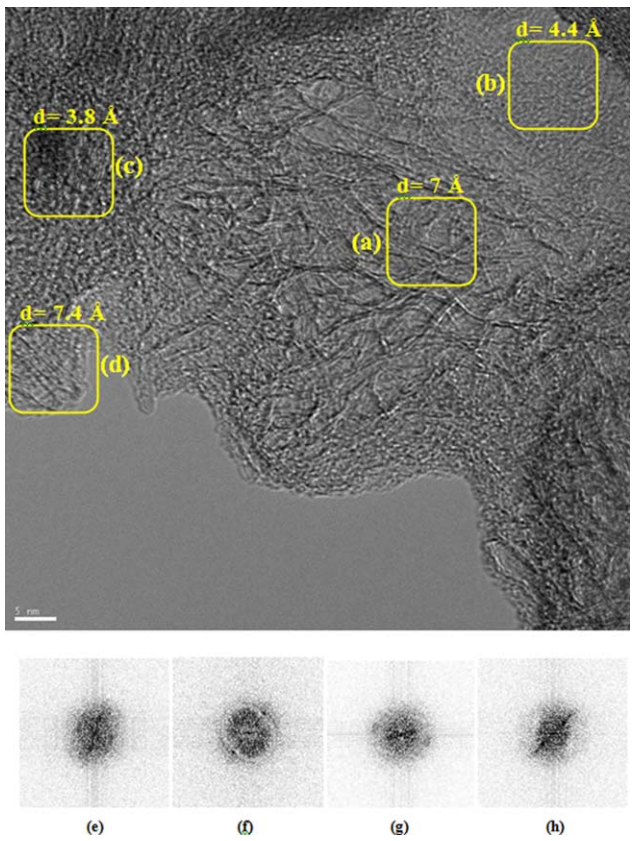

Figure 4. TEM micrograph of the copolymer. [Color figure can be viewed in the online issue, which is available at wileyonlinelibrary.com.]

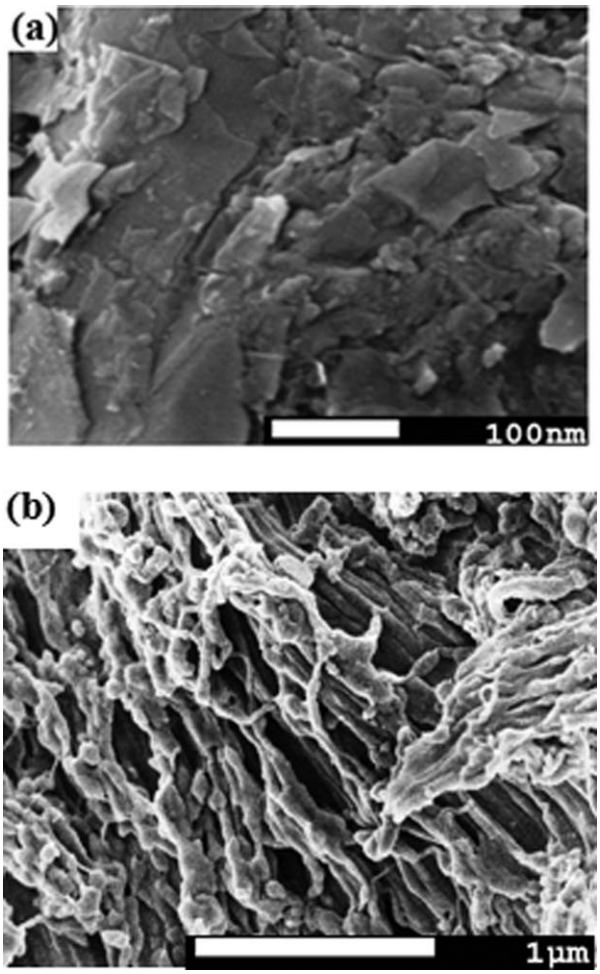

Figure 5. Scanning electron micrographs of (a) PVK and (b) copolymer.

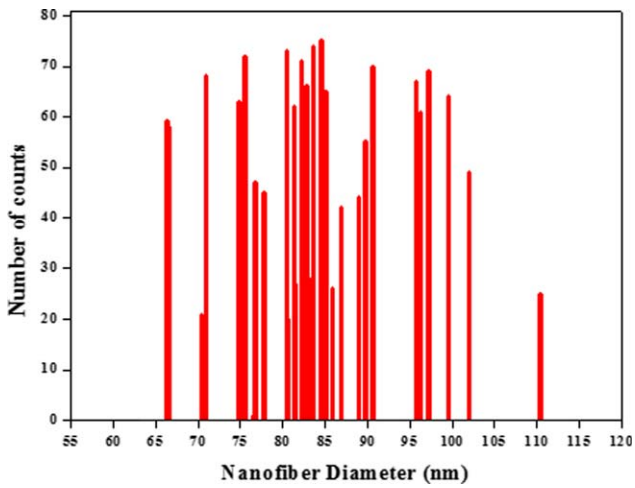

Figure 6. Histograms of appearing nanofibers diameters of the PVK-PPV copolymer. [Color figure can be viewed in the online issue, which is available at wileyonlinelibrary.com.]

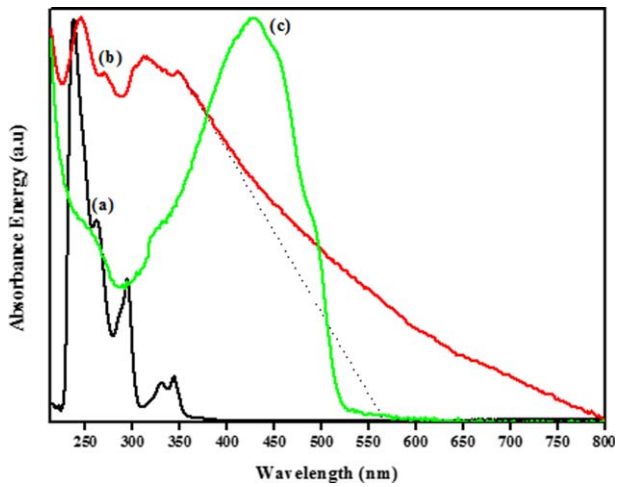

Figure 7. Optical absorption spectra of (a) PVK, (b) copolymer and (c) PPV. [Color figure can be viewed in the online issue, which is available at wileyonlinelibrary.com.]

The optical absorption spectra of the copolymer powder has been measured and compared to that PPV and PVK ones. All spectra shown in Figure 7 are normalized at the absorption maximum. For the copolymer, the UV part of the spectrum displays six separated bands located at 246, 270, 303, 315, 329 and 351 nm respectively. It is important to recall that the absorption spectrum of the PVK contains five bands located respectively at 232, at 260, at 294, at 330 and at 343 nm.[37] Referring to the absorption spectrum of the PVK novel features at 250, 275, nm and 315 nm appears for the copolymer. These new bands support the presence of the PPV segments in the copolymer backbone and their mixing with the VC units. For the visible part of the spectrum 400-800 nm, the optical absorption progressively decreases to zero in the case of copolymer without clear absorption edge, as for PPV. This monotonous variation can be attributed to a broad distribution of conjugated segments of PPV and it can also suggest that PPV segments with different lengths are present in the copolymer. Despite the lack of a sharp absorption decrease one can estimate an upper value for the electronic gap is found to be Eg = 2.2 eV, as deduced from the extrapolation of the slope of the spectrum between 350 and 400 nm. This gap is attributed to the $\pi \rightarrow \pi^{\star}$ electronic transitions of the carbon backbone. Referring to the PVK (3.6 eV) and PPV (2.7 eV) gaps, this value has been largely reduced, reflecting the insertion of conjugated segments of PPV.

The photoluminescence behavior of the copolymer has been investigated by stationary and time-resolved photoluminescence (PL). For the stationary case measured with an excitation line at 360 nm (Figure 8), a broad spectrum ranging from 400 to 750 nm is found. It is clear that this spectrum can definitely not be decomposed into a linear combination of the PVK and PPV spectra also reported in Figure 8. Indeed, the UV part between 350 and 400 nm is missing and the main band of the copolymer is located in a spectral region where the PL intensity of PVK and PPV is reduced. The copolymer spectrum can be fitted with six bands located at 417, 442, 470, 520 nm and 575 nm as shown in Figure 8. However in the case of the PPV, four bands -which constitute the spectrum- are located at 515, 550, 600 and 650 nm. In the case of PVK, the spectrum is constituted by three bands located at 389, 418, and 453 nm. It is clear, that the band at 418 nm—which present the maximum of luminescence of PVK—is located in the spectrum of copolymer as shown in Figure 8. In addition, it is important to note that the characteristics bands of PPV are present in the case of copolymer, which confirms the insertion of PPV units. On the other hand the redshift compared to the PVK implies an increase of the conjugation length. This increase results from the grafting of PPV units. Kinetically, this means that the exciton migration begins in the PVK backbone and continues in the PPV moiety. This is in good agreement with the FTIR results which proves the presence of dimeric carbazylium. The color of this new copolymer has been determined and reported on a *x,y* C.I.E. (Commission Internationale de l'Eclairage) Figure 9. It corresponds to a light blue color with $x = 0.196$ and $y = 0.227$. It can be noted that this color is approximately located between the deep blue of PVK and the green PPV.

3D-maps TR-PL in false colors for the PVK and copolymer are presented in Figure 10(a) using 3.1 eV (400 nm) as excitation energy. Figure 10(b) depicts the normalized PL intensity decays of the PVK and copolymer on a logarithmic scale in the range of 0-1ns. PL kinetics of PVK, copolymer and PPV, spectrally integrated between 300 nm and 700 nm. The PL normalized intensity decay times are very well simulated with two exponential decays and by taking into account the contribution of apparatus function including the Gaussian temporal dependence $G(t)$ of the laser pulse, as previously reported.[38]

$$\frac{dn_1}{dt} = G(t) - \beta_1 n_1 \quad (1)$$

$$\frac{dn_2}{dt} = G(t) - \beta_2 n_2 \quad (2)$$

where n_1 and n_2 are the populations of the excited states levels 1 and 2, their decay times τ_1 and τ_2 respectively. In this simple model,[38] the populations of levels 1 and 2 are coupled in order to account indirectly for a migration process from the short

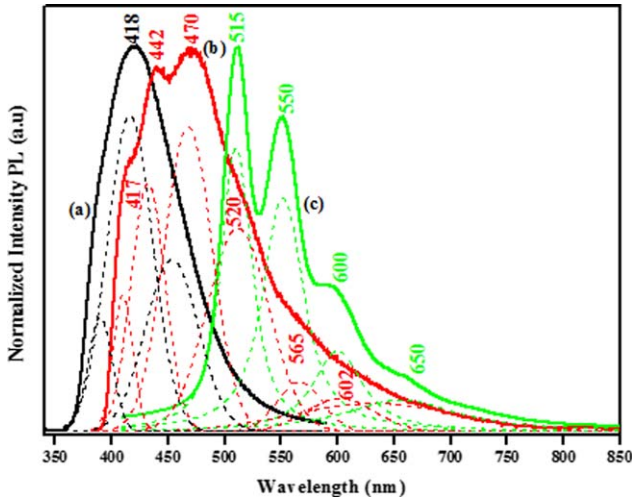

Figure 8. PL spectra of (a) PVK, (b) copolymer and (c) PPV. [Color figure can be viewed in the online issue, which is available at wileyonlinelibrary.com.]

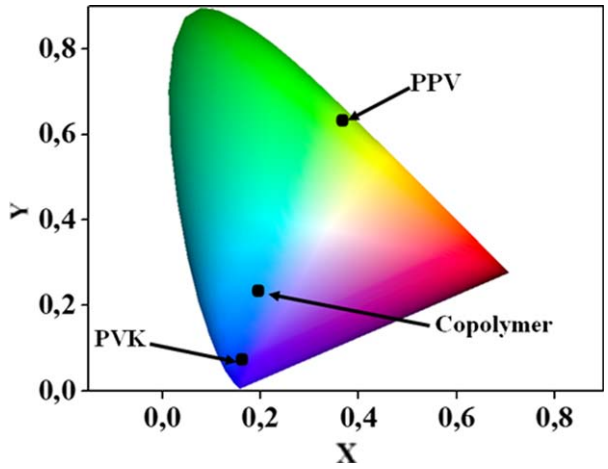

Figure 9. Chromaticity diagram (CIE coordinates) for PVK (x = 0.1575; y = 0.0814), Copolymer (x = 0.1964; y = 0.2272), and PPV (x = 0.3787; y = 0.5919) LEDs described. [Color figure can be viewed in the online issue, which is available at wileyonlinelibrary.com.]

to the long conjugated segments. These populations include photogenerated charges recombining radiatively and nonradiatively.

The decaying population is $n=A_1n_1+A_2n_2$, where A_1 and A_2 are proportional to the PL intensity from levels 1 and 2, respectively. We define below (eq. 3) an average decay time called τ_{mean} in order to show the average trend of the photogenerated charge migration time:

$$\tau_{mean}=\frac{(A_1\tau_1^2+A_2\tau_2^2)}{A_1\tau_1+A_2\tau_2} \quad (3)$$

The weight corresponding to the relative population of photogenerated charges contributing to each of the decay times (A_i, τ_i) is calculated by:

$$P_i(\%)=\frac{A_i\tau_i}{\sum A_i\tau_i}$$

Results are summarized in Table II. On one hand, from Table II, we have for the PVK τ_{mean}= 29.89 ns, with τ_1= 1.58 ns and τ_2= 33.41 ns. On the other hand, we also can see from Figure 9(b) that the decay times are shorter when going from PVK to the copolymer. For the copolymer, the decay time is close to the temporal resolution, and τ_{mean}= 0.36 ns obtained with τ_1= 0.09 ns and τ_2= 0.454 ns are few significant. However, referred to the PPV, the copolymer decay time is longer for the second excited level corresponding to

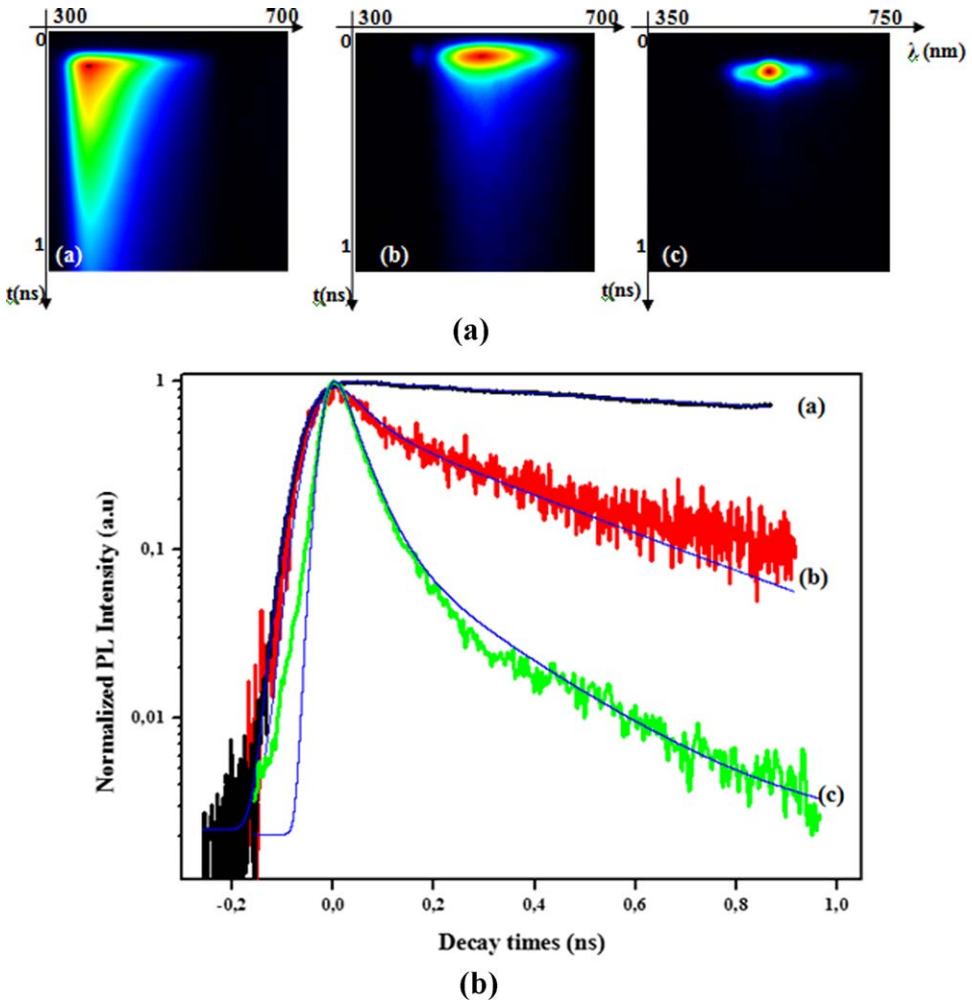

Figure 10. (a) The 3D-maps TR-PL in false colors of the PVK (a), of copolymer (b), and of PPV (c). (b) Time resolved photoluminescence spectra of: PVK (a), copolymer (b), and PPV (c). [Color figure can be viewed in the online issue, which is available at wileyonlinelibrary.com.]

Table II. Decay Times and Parameters (Defined in eq. 3) Deduced from the Analysis of the Experimental Photoluminescence Decay for PVK, Copolymer, and PPV

	P_1 (%)	P_2 (%)	τ_1 (ns)	τ_2 (ns)	τ_{mean} (ns)
PVK	11.05	88.95	1.58	33.41	29.89
Copolymer	24.75	75.25	0.09	0.45	0.36
PPV	29.50	70.50	0.04	0.21	0.15

recombinations on the longer chains. Consequently, the radiative processes become more important in copolymer compared with the PPV. In fact the value of τ_{mean} is doubled from PPV (about 0.15 ns) to the copolymer (about 0.36 ns). We can relate that at the morphology of copolymer which is more ordered and enhanced the facility of exciton migration. The exciton diffusion length is enhanced in case of copolymer it may be related the morphology structure.

The fractions of the photo-generated charge in the largest/shortest weighted segments represent respectively 70.50% and 29.50% for the PPV. In the case of copolymer these contributions are found to be 75.25% and 24.75%, respectively. Referring to the PPV, the increase of photo-generated charge populations in the long segments induces a longest in life time.

CONCLUSIONS

A new copolymer of poly(*N*-vinylcarbazole) and precursor of (PPV) was prepared by an oxidative way using the anhydrous $FeCl_3$. The successful synthesis of this new copolymer was confirmed by FTIR, SEM, TEM, optical absorption, and emission spectroscopy. Compared with the pristine polymer, the new condensed and organized matter reproducing the common properties of the PVK and the oligomeric PPV moieties showed higher thermal stability up to 450°C. The copolymer shows unique absorption and emission and a continuous donor acceptor existence. Accordingly, it seems to be promising constituent for photovoltaic devices application. Considering its emissive properties and nanofibers morphology, further understating and optimization of the multiple properties and applications are actually under study.

ACKNOWLEDGMENTS

The authors would like to thank F. LARI for assistance with synthesis assays and ATG analysis. The authors also wish to thank, M. PARIS for the NMR study, E. GAUTRON for TEM investigation, STEPHANT Nicolas for SEM study, J.Y. Mevellec for FTIR and Raman analysis and P.E. Pierre for XRD analysis and A. Garreau for its help and discussions and P. Bertoncini for characterization by micro-fluorescence under UV excitation.

REFERENCES

1. Zhang, W.; Yan, E.; Huang, Z.; Wang, C.; Xin, Y.; Zhao, Y.; Tong, Q. *Eur. Polym. J.* **2007**, *43*, 802.
2. Zhang, Z.; Wei, Z.; Wan, M. *Macromolecules* **2002**, *35*, 5937.
3. Djenizian, T.; Hanzu, I.; Eyraud, M.; Santinacci, L. C. R. *Chimie.* **2008**, *11*, 995.
4. Udum, Y. A.; Ergun, Y.; Sahin, Y.; Pekmez, K.; Yildiz, A. *J. Mater. Sci.* **2009**, *44*, 3148.
5. Hu, B.; Karasz, F. E. *J. Appl. Phys.* **2003**, *93*, 1995.
6. Jang. J. *Adv. In Polym. Sci.* **2006**, *199*, 189.
7. Yao, M.; Senoh, H.; Sakai, T.; Kiyobayashi, T. *J. Power Sources* **2012**, *202*, 364.
8. Star, A.; Lu, Y.; Bradley, K.; Grüner, G. **2004**, *9*, 1587.
9. Barlier, V.; Legaré, V. B.; Boiteux, G.; Davenas, J.; Slazak, A.; Rybak, A.; Jung, J. *Synth. Met.* **2009**, *159*, 508.
10. Yoon, S. J.; Chun, H.; Lee, M.; Kim, N. *Synth. Met.* **2009**, *159*, 518.
11. Yap, C. C.; Yahaya, M.; Salleh, M. M. *Curr. Appl. Phys.* **2009**, *9*, 722.
12. Sung, I. A.; Wan, K. K.; Si, H. R.; Kuk, J. K.; Seong, E. L.; Sung-Hoon, K.; Jung-Chul, P.; Kyung, C. C. *Org. El.* **2012**, *13*, 980.
13. Carmona, T.; Fernández-Peña, N.; Tarazona, E. S.; Mendicuti, F. *Eur. Polym. J.* **2010**, *46*, 1796.
14. Haldar, I.; Kundu, A.; Biswas, M.; Nayak, A. *Mater. Chem. Phys.* **2011**, *128*, 256.
15. Chemek, M.; Ayachi, S.; Hlel, A.; Wéry, J.; Lefrant, S.; Alimi, K. *Appl. Polym. Sci.* **2011**, *122*, 2391.
16. Li, H.; Termine, R.; Godbert, N.; Angiolini, L.; Giorgini, L.; Golemme, A. *Org. El.* **2011**, *12*, 1184.
17. Han, Y.; Wu, G.; Chen, H.; Wang, M. *J. Appl. Polym. Sci.* **2008**, *109*, 882.
18. Ballav, N.; Biswas, M. *Polym. Int.* **2004**, *53*, 198.
19. Ballav, N.; Biswas, M. *Synth. Met.* **2005**, *149*, 109.
20. Ballav, N.; Maity, A.; Biswas, M. *Mater. Chem. Phys.* **2004**, *87*, 120.
21. Chemek, M.; Wéry, J.; Bouachrine, M.; Paris, M.; Lefrant, S.; Alimi, K. *Synth. Met.* **2010**, *160*, 2306.
22. El Malki, Z.; Hasnaoui, K.; Bejjit, L.; Haddad, M.; Hamidi, M.; Bouachrine, M. *J. Non-Crys. Sol.* **2010**, *356*, 467.
23. Ballav, N.; Biswas, M. *Synth. Met.* **2003**, *132*, 213.
24. Burroughes, J. H.; Bradley, D. D. C.; Brown, A. R.; Marks, R. N.; Mackay, K.; Friend, R. H.; Burns, P. L.; Holmes, A. B. *Nature* **1987**, *347*, 539.
25. Jin, Y.; Song, S.; Park, S. H.; Park, J. A.; Kim, J.; Woo, H. Y.; Lee, K.; Suh, H. *Polymers* **2008**, *49*, 4559.
26. Xin, Y.; Lin, T.; Li, S.; Ling, Z.; Liu, G.; Huang, Z.; Lin J. *J. Lum.* **2012**, *132*, 738.
27. Vandenbergh, J.; Dergent, J.; Conings, B.; Krishna, T. V. V. G.; Maes, W.; Cleij, T. J.; Lutsen, L.; Manca, J.; Vanderzande, D. J. M. *Eur. Polym. J.* **2011**, *47*, 1827.
28. Herold, M.; Gmeimer, J.; Schwoerer, M. *Polym. Adv. Tech.* **1999**, *10*, 251.
29. Han, Y.; Wu, G.; Chen, H.; Wang, M. *J. Appl. Polym. Sci.* **2008**, *109*, 882.
30. Li, Y.; Yang, J.; Xu, J. *J. Elec. Chem.* **1995**, *399*, 79.
31. Gagnon, D. R.; Capistran, J. D.; Karasz, F. E.; Lenz, R. W. Antoun, S. *Polymers* **1987**, *28*, 567.

32. González, M. C.; Del Val, J. J.; Zamora, F. *Polymers* **2001**, *42*, 9735.

33. Chang, W.-P.; Whang, W.-T. *Polymers* **1996**, *37*, 3493.

34. Baibarac, M.; Lira-Cantu, M.; Oro Sol, J.; Baltog, I.; Casan-Pastor, N. *Comp. Sci. Tech.* **2007**, *67*, 2556.

35. Aarab, H.; Baîtoul, M.; Wéry, J.; Almairac, R.; Lefrant, S.; Faulques, E.; Duvail, J. L.; Hamedoun, M. *Synthetic Metals* **2005**, *155*, 63.

36. Teo, E. Y. H.; Ling, Q. D.; Song, Y.; Tan, Y. P.; Wang, W.; Kang, E. T.; Chan, D. S. H.; Zhu, C. *Organic Electron.* **2006**, *7*, 173.

37. Zaidi, B.; Bouzayen, N.; Wéry, J.; Alimi, K. *J. Mol. Str.* **2010**, *971*, 71.

38. Chemek, M.; Massuyeau, F.; Wéry, J.; Hlel, A.; Ayachi, S.; Faulques, E.; Lefrant, S.; Alimi, K. *J. Appl. Polym. Sci.* **2012**, *125*, 126.